Proceedings of the MCalv6(5) Conference

A. Elipe, J.I. Montijano and L. Rández (Editors)

2010

Numerical comparisons between Gauss-Legendre methods and Hamiltonian BVMs defined over Gauss points*

Luigi Brugnano

Dipartimento di Matematica "U. Dini", Università di Firenze, Italy

and

Felice Iavernaro, Tiziana Susca

Dipartimento di Matematica, Università di Bari, Italy

Dedicated to Prof.Manuel Calvo, on the occasion of his 65th birthday.

Abstract

Hamiltonian Boundary Value Methods are a new class of energy preserving one step methods for the solution of polynomial Hamiltonian dynamical systems. They can be thought of as a generalization of collocation methods in that they may be defined by imposing a suitable set of *extended collocation conditions.* In particular, in the way they are described in this note, they are related to Gauss collocation methods with the difference that they are able to precisely conserve the Hamiltonian function in the case where this is a polynomial of any high degree in the momenta and in the generalized coordinates. A description of these new formulas is followed by a few test problems showing how, in many relevant situations, the precise conservation of the Hamiltonian is crucial to simulate on a computer the correct behavior of the theoretical solutions.

1 Introduction

Hamiltonian Boundary Value Methods (HBVMs) form a subclass of Boundary Value Methods (BVMs), whose main feature is that of precisely conserving the Hamiltonian function associated with a canonical Hamiltonian system

$$\begin{cases} \dot{y} = J\nabla H(y), \\ y(t_0) = y_0 \in \mathbb{R}^{2m}, \end{cases} \qquad J = \begin{pmatrix} 0 & I \\ -I & 0 \end{pmatrix} \in \mathbb{R}^{2m \times 2m}, \tag{1}$$

(I is the identity matrix of dimension m), in the case where such function is of polynomial type.

Two key ideas have permitted the realization of HBVMs: the definition of *discrete line integral* and what we called *extended collocation conditions*. The former, first introduced in [15, 16], represents the discrete counterpart of the line integral defined over conservative vector fields, while the second is a relaxation of the classical collocation conditions which assures the conservation of the energy along the numerical solution $\{y_n\}$ generated by the method itself.

Just as an initial clarification, we briefly show how this new approach to the problem reads when the classical Gauss collocation method is considered (see [18, Remark 2.1] for more details). Given a stepsize $h > 0$ and a set of s abscissae $c_1 < \cdots < c_s$ disposed according to a Gauss-Legendre distribution on $[0, 1]$, the Gauss method of order $2s$ is defined by means of the following polynomial collocation problem:

$$\begin{cases} \sigma(t_0) = y_0, \\ \dot{\sigma}(t_0 + c_i h) = J\nabla H(\sigma(t_0 + c_i h)), \quad i = 1, \ldots, s. \end{cases} \tag{2}$$

As is well known, conditions (2) uniquely define a polynomial $\sigma(t)$ of degree s which is used to advance the solution by posing $y_1 = \sigma(t_0 + h)$, while the internal stages satisfy $Y_i = \sigma(t_0 + c_i h)$, $i = 1, \ldots s$. The coefficients of the Butcher array and the weights are given by

$$b_j = \int_0^1 \ell_j(c)\mathrm{d}c, \qquad a_{ij} = \int_0^{c_i} \ell_j(c)\mathrm{d}c, \qquad \text{with} \ \ \ell_j(c) = \prod_{r \neq j} \frac{c - c_r}{c_j - c_r}.$$

The s-degree polynomial $\sigma(t)$ may be thought of as a path in the phase space linking the state vectors y_0 to y_1 and passing through the stages $\{Y_i\}$. Due to the conservative nature of the vector field, we have that

$$H(y_1) - H(y_0) = \int_\sigma \nabla H(y) \cdot \mathrm{d}y = h \int_0^1 \dot{\sigma}(t_0 + \tau h)^T \nabla H(\sigma(t_0 + \tau h))\mathrm{d}\tau. \tag{3}$$

Now, the above integral is exactly computed by the Gauss quadrature formula with abscissae $\{c_i\}$ and weights $\{b_i\}$ if the degree of the integrand is not greater than $2s - 1$ which means that the degree of $H(y)$, say ν, must not exceed 2 (linear or quadratic Hamiltonians only). Under this assumption, taking into account the collocation conditions (2), we obtain

$$\begin{aligned} H(y_1) - H(y_0) &= h \sum_{i=1}^s b_i (\dot{\sigma}(t_0 + c_i h))^T \nabla H(\sigma(t_0 + c_i h)) \\ &= -h \sum_{i=1}^s b_i \nabla^T H(\sigma(t_0 + c_i h)) J \nabla H(\sigma(t_0 + c_i h)) = 0. \end{aligned} \tag{4}$$

Thus, by following a different route, we have obtained the classical result that the Gauss methods conserve quadratic Hamiltonian functions while fail to conserve polynomial Hamiltonian functions of higher degree.[1]

---

[1] This argument may be generalized to other classes of collocation methods.

The above example is the starting point of our approach: the *discrete line integral* is the first sum in (4), which turns out to vanish for quadratic Hamiltonians, due to the collocation conditions (2).

The next section reports a descriptive introduction to HBVMs with much emphasis to the key ideas they rely on. We refer the reader to the papers [3, 4, 18, 2, 5, 13, 14, 1] for the details about the basic theory and implementation of HBVMs, and to the monograph [6] as a reference for the theory of BVMs.

In Section 3 we report a number of test problems of some relevance in the literature, for which the precise conservation of the energy turns out to be a crucial feature for the correct reproduction of the long time behavior of the solutions. This will be testified by comparing HBVMs to the Gauss method which, by the way, is a symplectic integrator.

2   Hamiltonian Boundary Value Methods

In this section we introduce HBVMs by slightly elaborating the arguments in [3, 4, 5]. As was said above, the basic idea which HBVMs rely on is the so called discrete line integral, which is the discrete counterpart of the line integral associated with a conservative vector field. In more detail, starting from (3), we consider a polynomial, of degree at most s, such that

$$\sigma(t_0) = y_0, \qquad \sigma(t_0 + h) = y_1, \tag{5}$$

providing an approximation to the solution on the interval $[t_0, t_0 + h]$. We consider the following expansions,

$$\dot\sigma(t_0 + \tau h) = \sum_{j=1}^{s} P_j(\tau)\gamma_j, \qquad \sigma(t_0 + \tau h) = y_0 + h\sum_{j=1}^{s} \int_0^{\tau} P_j(x)\mathrm{d}x\, \gamma_j, \tag{6}$$

where the (vector) coefficients $\{\gamma_i\}$ are to be determined. We also assume that the polynomials $\{P_i\}$ constitute an orthonormal basis, on the interval $[0, 1]$, for the vector space Π_{s-1} of polynomials of degree at most $s - 1$, i.e.,

$$\int_0^1 P_i(\tau)P_j(\tau) = \delta_{ij}, \qquad i, j = 1, \ldots, s.$$

Such polynomials can be easily obtained by a suitable scaling of the shifted Legendre polynomials [5]. Substitution of the first expansion in (6) into the line integral in (3), which we require to vanish, then gives

$$\sum_{j=1}^{s} \gamma_j^T \int_0^1 P_j(\tau)\nabla H(\sigma(t_0 + \tau h))\mathrm{d}\tau = 0,$$

which is certainly satisfied by choosing

$$\gamma_j = \int_0^1 P_j(\tau) J \nabla H(\sigma(t_0 + \tau h)) \mathrm{d}\tau, \qquad j = 1, \ldots, s. \tag{7}$$

Multiplication of (7) by $h \int_0^c P_j(x) \mathrm{d}x$ and summation over j then gives, by virtue of the second expansion in (6),

$$\sigma(t_0 + ch) = y_0 + h \sum_{j=1}^s \int_0^c P_j(x) \mathrm{d}x \int_0^1 P_j(\tau) J \nabla H(\sigma(t_0 + \tau h)) \mathrm{d}\tau, \qquad c \in [0, 1]. \tag{8}$$

Let us now assume that $H(y)$ is a polynomial of degree ν. Consequently, the integral appearing at the right-hand side in (8) can be exactly discretized by a Gaussian formula over k Gauss-Legendre abscissae $\{c_i\}$, which we shall consider hereafter, provided that

$$k \geq \frac{\nu s}{2}. \tag{9}$$

Let us denote by $\{\omega_i\}$ the weights of the quadrature formula, and set

$$y_i = \sigma(t_0 + c_i h), \quad a_{ij} = \int_0^{c_i} P_j(x) \mathrm{d}x, \qquad i = 1, \ldots, k, \quad j = 1, \ldots, s. \tag{10}$$

Consequently, (8) can be (exactly) discretized as:

$$y_i = y_0 + h \sum_{j=1}^s a_{ij} \sum_{\ell=1}^k \omega_\ell P_\ell(c_\ell) J \nabla H(y_\ell), \qquad i = 1, \ldots, k. \tag{11}$$

Definition 2.1 *The set of equations (11), to be solved for the unknowns $\{y_i\}$, defines an HBVM with k steps and degree s, in short HBVM(k, s).*

For such method, the following properties hold true [4]:

- it has order $2s$ for all $k \geq s$;

- it is symmetric and perfectly A-stable (i.e., its stability region coincides with the left-half complex plane, $\mathbb{C}^-$ [6]);

- for $k = s$, it reduces to the Gauss-Legendre method of order $2s$;

- it exactly preserves polynomial Hamiltonian functions of degree ν, provided that (9) holds true.

Remark 2.2 *The actual implementation of HBVM(k, s) can be seen to result in the solution of a system of (block) size s, whatever is the value of k considered [3, 5]. Consequently, if needed, large values of k can be easily considered.*

The arguments in the previous remark, allow us to consider the limit formula of (10)–(11), in the case where $H(y)$ is non-polynomial, as $k \to \infty$. Clearly such a limit is given by formula (8), which, according to [4], is named *HBVM(∞, s)* or *∞-HBVM of degree s*.

However, we emphasize that formula (8) becomes an operative method only after that a suitable discretization of the inner integral is considered and, replacing the integral by a quadrature formula with k nodes, leads back to a HBVM(k, s) method.

One can easily argue that, since in the non polynomial case the quadrature formula can approximate the corresponding integral with an arbitrary accuracy, under suitable regularity assumptions for $H(y)$, a *practical* conservation of the energy may be obtained [4, 17]. The term "practical" means that, in many general situations, when k is high enough, the method makes no distinction between the function $H(y)$ and its polynomial approximation, being the latter in a neighborhood of size ε of the former, where ε denotes the machine precision.

We end this section by observing that, by differentiating both members of (8), one obtains

$$\dot{\sigma}(t_0 + ch) = \sum_{j=1}^{s} P_j(c) \int_0^1 P_j(\tau) J \nabla H(\sigma(t_0 + \tau h)) \mathrm{d}\tau, \qquad c \in [0, 1],$$

which at the points $\{c_i\}$ provides, assuming $H(y)$ to be a polynomial and k large enough:

$$\dot{\sigma}(t_0 + c_i h) = \sum_{j=1}^{s} P_j(c_i) \int_0^1 P_j(\tau) J \nabla H(\sigma(t_0 + \tau h)) \mathrm{d}\tau, \qquad i = 1, \dots, k.$$

Such formulae (the former being the limit of the latter as $k \to \infty$) can be regarded as a kind of *extended collocation conditions* that generalize conditions (2), according to [18, Section 2] (see also [4]).

3   Numerical tests

We present a few numerical test highlighting the good behavior of HBVMs in the long-time simulation of Hamiltonian systems. A direct comparison of HBVMs with Gauss methods is reported in order to better emphasize the stability properties of the former methods even when compared to a well known class of symplectic formulae.[2]

The use of a large stepsize of integration is a prerogative in long-time simulation of an evolutionary problem but, in general, one is forced to reduce h under a critical threshold in order to guarantee the qualitative behavior of the theoretical solution to be well reproduced by the numerical solution. From this point of view, we show that HBVMs

---

[2]As was seen in the previous section, the choice of Gauss methods has also been dictated by the fact that they represent the *generating* formulae of HBVMs when we use a Gauss distribution of the abscissae, namely the Gauss method of order $2s$ coincides with HBVM(s,s).

allow the use of larger stepsizes than Gauss methods, which states that the conservation of the Hamiltonian function plays an important role in detecting the correct topological features of the solutions.

3.1 Sitnikov's problem

One of the main problems in Celestial Mechanics is to describe the motion of N point particles of positive mass $\{m_i\}$ moving under Newton's law of gravitation when we know their positions $\{q_i\}$ and momenta $\{p_i\}$ at a given time. Such a dynamical system, called the N-body problem, is in the form (1), with Hamiltonian

$$H(\boldsymbol{q}, \boldsymbol{p}) = \frac{1}{2} \sum_{i=1}^{N} \frac{||p_i||_2^2}{m_i} - G \sum_{i=1}^{N} m_i \sum_{j=1}^{i-1} \frac{m_j}{||q_i - q_j||_2}, \tag{12}$$

with G the gravitational constant. While the two-body problem is completely solved in the sense that we can describe explicitly all its solutions (see, e.g., [12]), this is no more the case, for $N \geq 3$. Consequently, numerical simulation is of interest, in such a case.

The Sitnikov problem is a particular configuration of the 3-body dynamics. In this problem two bodies of equal mass (primaries) revolve about their center of mass, here placed at the origin, in elliptic orbits in the (x, y)-plane. A third, and much smaller body (planetoid), is placed on the z-axis with initial velocity parallel to this axis as well.

The third body is small enough that the two body dynamics of the primaries is not destroyed. Then, the motion of the third body will be restricted to the z-axis and oscillating around the origin but not necessarily periodic. In fact, this problem has been shown to exhibit a chaotic behavior when the eccentricity of the orbits of the primaries exceeds a critical value that, for the data set we have used, is $\bar{e} \simeq 0.725$ (see Figure 1).

We have solved the Kepler problem with Hamiltonian function (12) by the Gauss method of order 4 (HBVM(2,2)) and by HBVM(18,2) (order 4 and 18 steps), with the following set of parameters:

N	G	m_1	m_2	m_3	e	d	h	$t_{\max}$
3	1	1	1	10^{-5}	0.75	5	0.5	1500

where e is the eccentricity, d is the distance of the apocentres of the primaries (points at which the two bodies are the furthest), h is the time-step and $[0, t_{\max}]$ is the time integration interval. The eccentricity e and the distance d may be used to define the initial condition $\boldsymbol{y}_0 = [\boldsymbol{q}_0, \boldsymbol{p}_0]$ (see [19] for the details):

$$\boldsymbol{q}_0 = [-\tfrac{5}{2},\ 0,\ 0,\ \tfrac{5}{2},\ 0,\ 0,\ 0,\ 0,\ 10^{-9}],$$
$$\boldsymbol{p}_0 = [0,\ -\tfrac{1}{20}\sqrt{10},\ 0,\ 0,\ \tfrac{1}{20}\sqrt{10},\ 0,\ 0,\ 0,\ \tfrac{1}{2}].$$
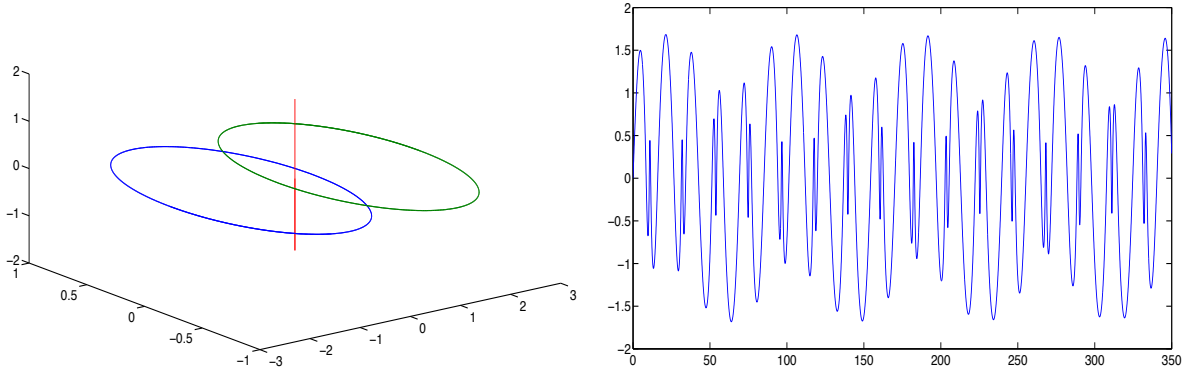
Figure 1.— The left picture displays the configuration of 3-bodies in the Sitnikov problem. To an eccentricity of the orbits of the primaries $e = 0.75$, there correspond bounded chaotic oscillations of the planetoid as is argued by looking at the space-time diagram in the right picture.
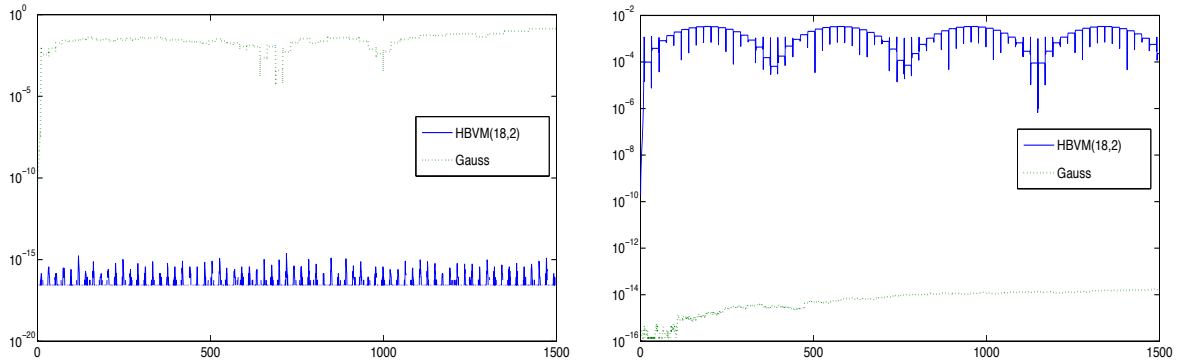

Figure 2.— Left picture: relative error $|H(y_n) - H(y_0)|/|H(y_0)|$ of the Hamiltonian function evaluated along the numerical solution of the HBVM(18,2) and the Gauss method. Right picture: relative error $|M(y_n) - M(y_0)|/|M(y_0)|$ of the angular momentum evaluated along the numerical solution of the HBVM(18,2) and the Gauss method.

First of all, we consider the two pictures in Figure 2 reporting the relative errors in the Hamiltonian function and in the angular momentum evaluated along the numerical solutions computed by the two methods. According to (9), we know that the HBVM(18,2) precisely conserves Hamiltonian polynomial functions of degree at most 18. This accuracy is high enough to guarantee that the nonlinear Hamiltonian function (12) is as well conserved up to the machine precision (see the left picture): from a geometrical point of view, this means that a local approximation of the level curves of (12) by a polynomial of degree 18 leads to a negligible error. The Gauss method exhibits a certain error in the Hamiltonian function while, being this formula symplectic, it precisely conserves the angular momentum, as is confirmed by looking at the right picture of Figure 2. From the same picture, one sees that the error in the numerical angular momentum associated with the HBVM(18,2) undergoes some bounded periodic-like oscillations.

Figures 3 and 4 show the numerical solution computed by the Gauss method and
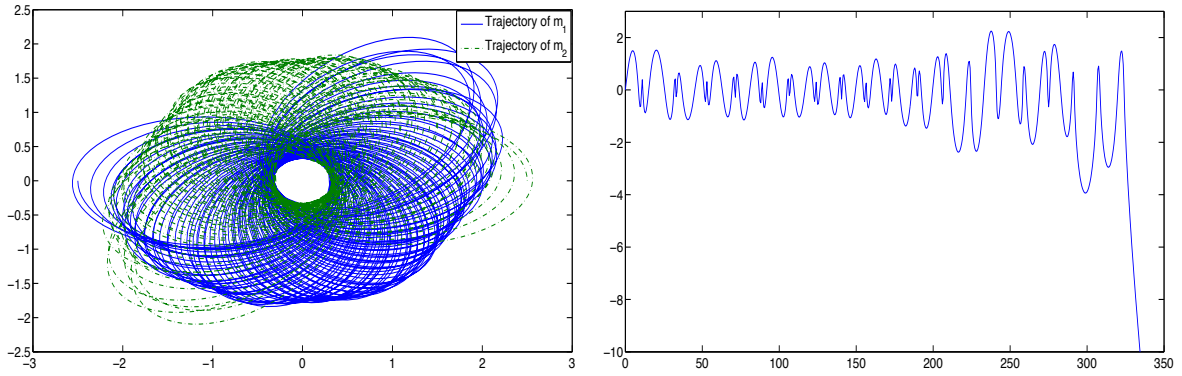
Figure 3.— The Sitnikov problem solved by the Gauss method of order 4, with stepsize $h = 0.5$, in the time interval $[0, 1500]$. The trajectories of the primaries in the (x, y)-plane (left picture) exhibit a very irregular behavior which causes the planetoid to eventually leave the system, as illustrated by the space-time diagram in the right picture.
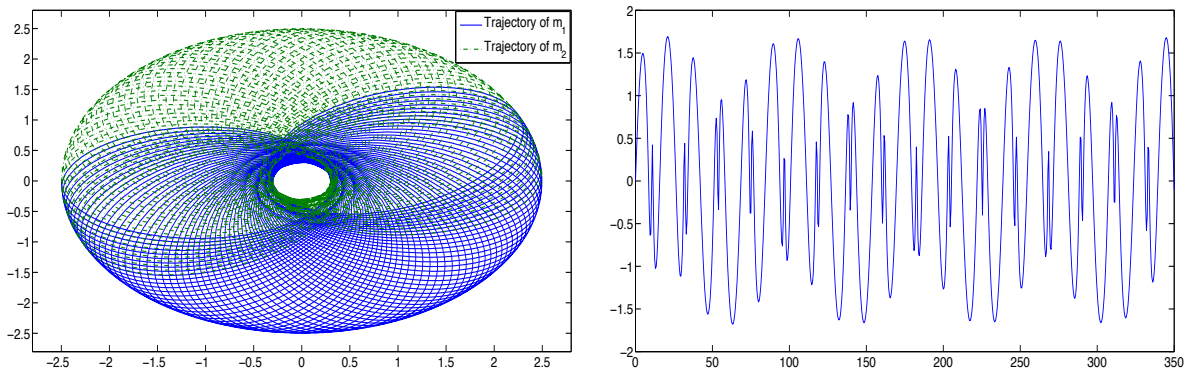

Figure 4.— The Sitnikov problem solved by the HBVM(18,2) method (order 4), with stepsize $h = 0.5$, in the time interval $[0, 1500]$. Left picture: the trajectories of the primaries are ellipse shape. The discretization introduces a fictitious uniform rotation of the (x, y)-plane which, however, does not alter the global symmetry of the system. Right picture: the space-time diagram of the planetoid on the z-axis displayed (for clearness) on the time interval $[0, 350]$ shows that, although a large value of the stepsize h has been used, the overall behavior of the dynamics is well reproduced (compare with the right picture of Figure 1).

HBVM(18,2), respectively. Since the methods leave the (x, y)-plane invariant for the motion of the primaries and the z-axis invariant for the motion of the planetoid, we have just reported the motion of the primaries in the (x, y)-phase plane (left pictures) and the space-time diagram of the planetoid (right picture).

We observe that, for the Gauss method, the orbits of the primaries are irregular in character so that the third body, after performing some oscillations around the origin, will eventually leave the system (see the right picture of Figure 3). On the contrary (left picture of Figure 4), the HBVM(18,2) generates a quite regular phase portrait. Due to the large stepsize h used, a sham rotation of the (x, y)-plane appears which, however, does
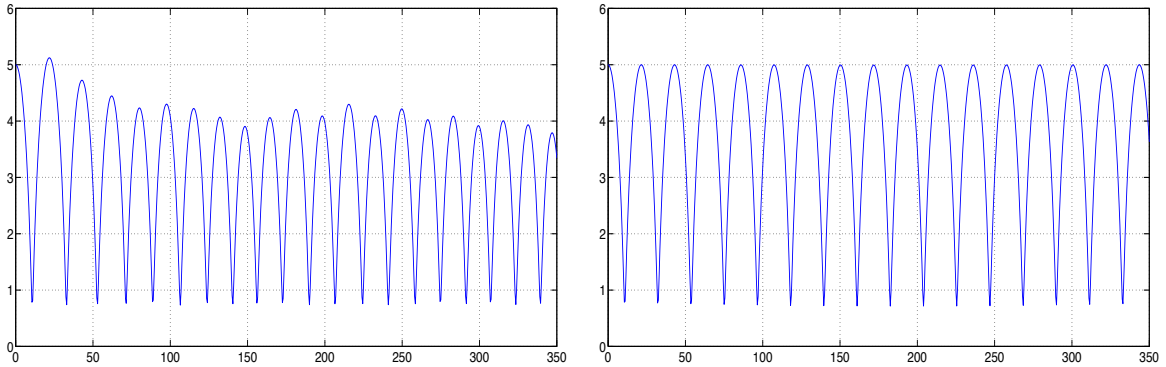
Figure 5.— Distance between the two primaries as a function of the time, related to the numerical solutions generated by the Gauss method (left picture) and HBVM(18,2) (right picture). The maxima correspond to the distance of apocentres. These are conserved by HBVM(18,2) while the Gauss method introduces patchy oscillations that destroy the overall symmetry of the system.

not destroy the global symmetry of the dynamics, as testified by the bounded oscillations of the planetoid (right picture of Figure 4) which look very similar to the reference ones in Figure 1. This aspect is also confirmed by the pictures in Figure 5, displaying the distance of the primaries as a function of the time. We see that the distance of the apocentres (corresponding to the maxima in the plots), as the two bodies wheel around the origin, are preserved by the HBVM(18,2) (right picture) while the same is not true for the Gauss method (left picture).

3.2 The Hénon-Heiles problem

The Hénon-Heiles equation originates from a problem in Celestial Mechanics describing the motion of a star under the action of a gravitational potential of a galaxy which is assumed time-independent and with an axis of symmetry (the z-axis) (see [11] and references therein). The main question related to this model was to state the existence of a third first integral, beside the total energy and the angular momentum.[3] By exploiting the symmetry of the system and the conservation of the angular momentum, Hénon and Heiles reduced from three (cylindrical coordinates) to two (planar coordinates) the degrees of freedom, thus showing that the problem was equivalent to the study of the motion of a particle in a plane subject to an arbitrary potential $U(q_1, q_2)$:

$$H(\boldsymbol{q}, \boldsymbol{p}) = \frac{1}{2}(p_1^2 + p_2^2) + U(q_1, q_2). \qquad (13)$$

Since U in (13) has no symmetry in general, we cannot consider the angular momentum as an invariant anymore, so that the only known first integral is the total energy

---

[3] An analytical approach to the problem may be found in [10], where the author finds out a formal expansion of the third invariant.
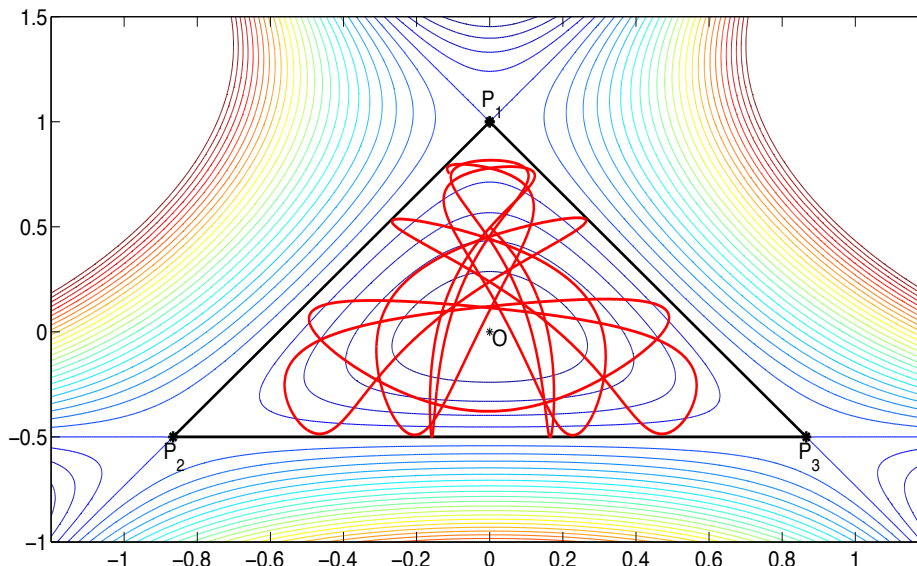
Figure 6.— Level curves of the potential $U(q_1, q_2)$ of the Hénon-Heiles problem (see (14)). The origin O is a stable equilibrium point, whose domain of stability contains the equilateral triangle having as vertices the saddle points P_1, P_2, and P_3, provided that the total energy does not exceed the value $\frac{1}{6}$. Inside the triangle an orbit $(q_1(t), q_2(t))$ is traced whose total energy is close (but lower than) $\frac{1}{6}$. The trajectory gets very close to the sides of the triangle, which makes the problem of conserving the total energy in the numerical solution an important feature to avoid instability when a large stepsize is used.

represented by (13) itself, and the question is whether or not a second integral does exist. Hénon and Heiles conducted a series of tests with the aim of giving a numerical evidence of the existence of such integral for moderate values of the energy H, and of the appearance of chaotic behavior when $H(\boldsymbol{q}, \boldsymbol{p})$ becomes larger than a critical value. In particular, for their experiments they choose

$$U(q_1, q_2) = \frac{1}{2}(q_1^2 + q_2^2) + q_1^2 q_2 - \frac{1}{3} q_2^3, \tag{14}$$

which makes the Hamiltonian function a polynomial of degree three.

When $U(q_1, q_2)$ approaches the value $\frac{1}{6}$, the level curves of U tend to an equilateral triangle, whose vertices are saddle points of U (see Figure 6). This vertices have coordinates $P_1 = (0, 1)$, $P_2 = (-\frac{\sqrt{3}}{2}, -\frac{1}{2})$ and $P_3 = (\frac{\sqrt{3}}{2}, -\frac{1}{2})$.

We consider an initial point $(\boldsymbol{q}_0, \boldsymbol{p}_0)$ such that $\boldsymbol{q}_0$ is inside the triangle $U \leq \frac{1}{6}$ and $H(\boldsymbol{q}_0, \boldsymbol{p}_0) < \frac{1}{6}$: then the orbit originating from $(\boldsymbol{q}_0, \boldsymbol{p}_0)$ will never abandon the triangle for any value of the time t. However, when $H(\boldsymbol{q}_0, \boldsymbol{p}_0)$ is chosen very close to $\frac{1}{6}$, a numerical method which does not preserve exactly the total energy could cause the (numerical) orbit to jump outside the triangle and possibly to diverge to infinity. This aspect is further emphasized when a large stepsize of integration is used, as is usually required in the long time simulation of a dynamical system.
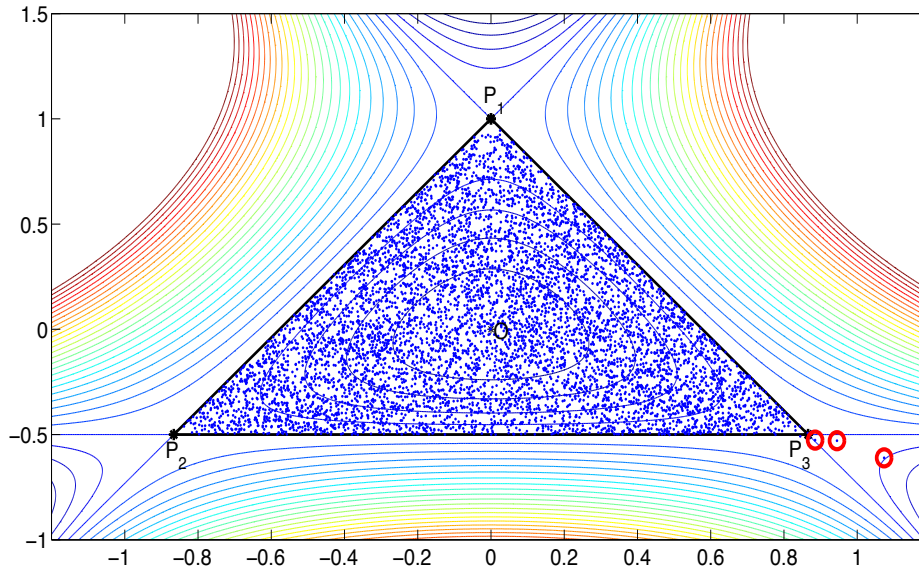
Figure 7.— The numerical trajectory in the (q_1, q_2)-plane computed by the Gauss method of order four with stepsize $h = 1$. The stable character of the continuous orbit is not correctly reproduced by the numerical method: after a time $t \simeq 7000$ the orbit escapes from the triangle (see the dots surrounded by small circles at the bottom right of the picture).

We have integrated problem (13) in the time interval $[0, 5 \cdot 10^4]$ with stepsize $h = 1$ by using the Gauss method of order four (HBVM(2,2)) and the HBVM(4,2) method which assures an exact conservation of the total energy.

Figures 7 and 8 show the numerical trajectories in the (q_1, q_2)-plane as dots that eventually will densely fill the triangle. The orbit generated by the Gauss method is plotted up to time $t \simeq 7000$, since it then escapes from the triangle, as highlighted by the three circles close to the saddle point P_3. In fact, as Figure 9 shows, the numerical Hamiltonian function associated with the Gauss method produces very irregular oscillations around the theoretical value (straight line) which eventually determine a loss of stability.

On the contrary, all the 50000 dots of the numerical trajectory computed by the HBVM(4,2) method are visible in Figure 8.

3.3 Computing the period annulus of a non-degenerate center of a polynomial Hamiltonian planar system.

Non-degenerate centers[4] of planar, in particular polynomial, Hamiltonian systems are extensively researched in the modern literature (see [9, 7, 22, 8] and references therein). The integration of such systems by means of HBVMs deserves a particular interest because, the degrees of freedom being one, the corresponding numerical solution is guaran-

---

[4] We recall that a center is an equilibrium point which is surrounded by periodic orbits. It is *non-degenerate* if the linearized vector field at this point has non-zero eigenvalues.
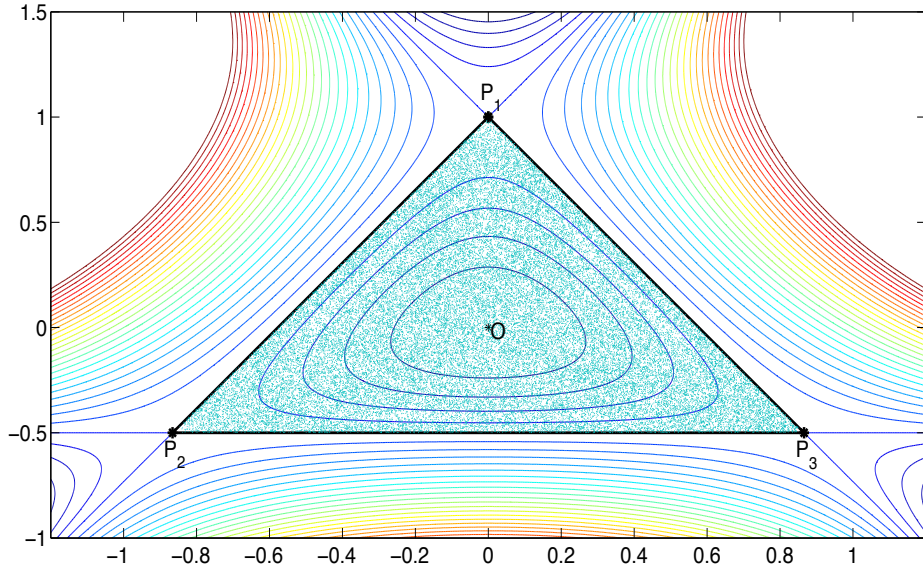
Figure 8.— The numerical trajectory in the (q_1, q_2)-plane computed by the HBVM(4,2) method with stepsize $h = 1$. Since this method precisely conserves the total energy of the system, the orbit is entirely contained in the triangle at all times.

teed to lie on the same level set $H(q, p) = H(q_0, p_0)$ as the theoretical orbit. Furthermore, if this latter consists of a closed orbit surrounding an equilibrium point (center), the numerical solution will (in general) fill densely the corresponding closed level curve, thus reproducing the very same phase portrait associated with the original continuous problem.

The region of marginal stability of a center P_0, is called the *period annulus of P_0* and will be denoted by $\mathcal{P}$: it is the largest punctured neighborhood of the center consisting of only periodic orbits. The function which associates to any periodic orbit in $\mathcal{P}$ its period is called the *period function* of the center. Such function has been being intensively studied for many years: its behavior relates to problems of isochronicity,[5] monotonicity, bifurcation of its critical points, etc.

The aim of the present example is to consider one such system and try to reproduce numerically, as best as possible, the set $\partial \mathcal{P}$, that is the boundary of the period annulus $\mathcal{P}$. Let $H^* < +\infty$ be the value of the Hamiltonian function corresponding to any points on $\partial \mathcal{P}$.[6] The Hamiltonian function we consider here is the fifth-degree polynomial

$$H(p, q) = A(p) + B(p)q + C(p)q^2 + D(p)q^3, \tag{15}$$

where

$$A(p) = p^2(\tfrac{1}{2} + c_3 p + b_3 p^2 + a_3 p^3), \qquad B(p) = p^2(c_2 + b_2 p + a_2 p^2),$$
$$C(p) = \tfrac{1}{2} + c_1 p + b_1 p^2 + a_1 p^3, \qquad D(p) = c_0 + b_0 p + a_0 p^2,$$

---

[5] Namely, all the orbits surrounding the center P_0 share the same period.

[6] Here we assume that the center P_0 is non global: this is certainly true if $H(q, p)$ is a polynomial of odd degree.
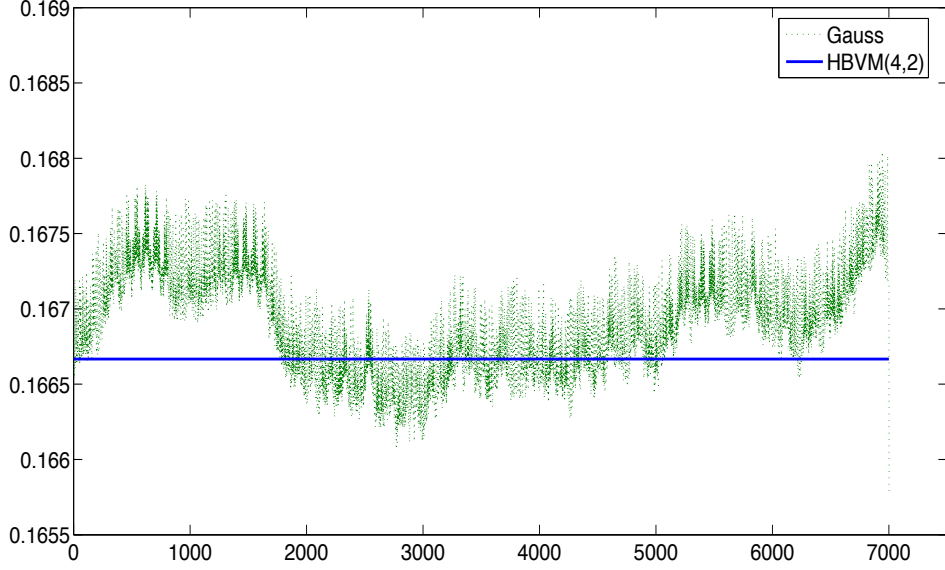
Figure 9.— Hamiltonian function evaluated along the numerical solution of the Gauss and HBVM(4,2) methods. The irregular oscillations introduced by the Gauss method will cause the associated numerical solution to eventually leave the stability region centered at the origin.

with $(a_0, a_1, a_2, a_3) \neq (0,0,0,0)$.[7] Note that, since $H(q,p) = \frac{1}{2}(p^2 + q^2) + $ h.o.t., we can assume P_0 to be the origin $O = (0,0)$.

The class of Hamiltonian systems defined by (15) has been proposed in [20] and [21].[8] Their main result was proving that the origin may not be an isochronous center [20] and, more specifically, that the period tends to infinity as $H(q_0, p_0) \nearrow H^*$, (q_0, p_0) being the initial condition associated with the differential system.

For our experiments, we have set the values of the coefficients $\{a_i\}$, $\{b_i\}$, and $\{c_i\}$ as follows:

$$a_0 = 0; \qquad a_1 = 0; \qquad a_2 = 1; \qquad a_3 = 0;$$
$$b_0 = 0; \qquad b_1 = 1; \qquad b_2 = 0; \qquad b_3 = 1; \qquad (16)$$
$$c_0 = 0; \qquad c_1 = 1; \qquad c_2 = 1; \qquad c_3 = 0.$$

In such a case, besides the origin $P_0 = (0,0)$, $H(q,p)$ admits the following real equilibrium points (up to the machine precision):

$$P_1 = (-6.879526475540134 \cdot 10^{-1}, \ -5.206527058470621 \cdot 10^{-1}) \longrightarrow \text{saddle point;}$$
$$P_2 = (-1.179582379893681, \ 1.756351969248087) \longrightarrow \text{saddle point.}$$

---

[7] Otherwise the degree of $H(q,p)$ becomes lower than 5.

[8] The authors showed that, without loss of generality, the form (15) may be associated to any polynomial Hamiltonian system of degree four and admitting a non-degenerate center, via a suitable change of coordinates.

Figure 10 reports the shape of the level curves of (15)–(16) in a region enclosing P_0 and P_1. We see that the limit closed orbit corresponding to $\partial \mathcal{P}$ is the one embracing P_0 and having P_1 as both ω-limit point and α-limit point[9] and, therefore, the value H^* may be computed with precision as

$$H^* = H(P_1) = 9.050199350868576 \cdot 10^{-2}. \tag{17}$$

Now suppose we do not know the value H^* in (17) (it will be used as a reference value) and that we want to reproduce the orbit covering $\partial \mathcal{P}$ by simply picking initial points (q_0, p_0) further and further away from the origin, and checking whether the numerical solution remains bounded over a long time.[10] More precisely, we will locate the limit cycle by means of a dichotomic search, according to the following algorithm:

step 1: find a point Q from which an orbit originates that does not embraces the critical point P_0 (that is $Q \notin \mathcal{P}$);

step 2: consider the segment joining P_0 to Q:
$$\gamma(c) = (1 - c)P_0 + cP_1, \qquad c \in [0, 1],$$
and set $c_0 = 0$ and $c_1 = 1$;

step 3: if $c_1 - c_0 < \text{tol}$, STOP   (tol is a specified tolerance);

step 4: set $c = \frac{c_0 + c_1}{2}$ and solve numerically the Hamiltonian problem defined in (15), considering $\gamma(c)$ as initial condition, in the time interval $[0, hN]$ where $h > 0$ is the stepsize and N is a positive integer such that hN is large enough to give some information about the fate of the orbit originating from $\gamma(c)$.

step 5: if the numerical solution eventually depart from P_0, set $c_1 = c$, otherwise set $c_0 = c$, go to step 3;

The point $y_0 \equiv (q_0, p_0) = \gamma(c)$, where c is the value resulting after the execution of the above procedure, may be assumed as a point on $\partial \mathcal{P}$ within the specified tolerance tol. Detecting the limit cycle with high accuracy requires a huge number of simulations and therefore large run times, also taking into account the wide time intervals that must be used in order to inspect the asymptotic behavior of the numerical solution.[11] Consequently, it would be advisable to work with a relatively large stepsize h. We have set:

$$h = 1, 0.5, \quad N = 2500, 5000, \quad \text{tol} = 2^{-52} \text{ (i.e., the value of \texttt{eps} in Matlab)}, \quad Q = (0, 1),$$

to cover the integration interval $[0, 2500]$.

---

[9] That is, $\lim_{t \to \pm \infty} (q(t), p(t)) = P_1$ for any choice of $(q_0, p_0) \in \partial P$.

[10] Of course, we cannot assume $(q_0, p_0) = P_1$ since P_1 is an equilibrium point.

[11] Actually, by virtue of their conservation properties, HBVMs do not need to be integrated over a long time, even though here we do that for comparison purposes.

h	s	a point $y_0^{(s,s)} \in \partial\mathcal{P}$ computed by the Gauss method	$\frac{|H(y_0^{(s,s)})-H^*|}{H^*}$	a point $y_0^{(k,s)} \in \partial\mathcal{P}$ computed by HBVM(k,s)	$\frac{|H(y_0^{(k,s)})-H^*|}{H^*}$
1	2	$(0,\ 3.723580509957994 \cdot 10^{-1})$	$2.15 \cdot 10^{-2}$	$(0,\ 3.757055929263451 \cdot 10^{-1})$	$7.66 \cdot 10^{-16}$
	3	$(0,\ 3.748759009745006 \cdot 10^{-1})$	$5.38 \cdot 10^{-3}$	$(0,\ 3.757055929263451 \cdot 10^{-1})$	$4.60 \cdot 10^{-16}$
	4	$(0,\ 3.754691919292651 \cdot 10^{-1})$	$1.53 \cdot 10^{-3}$	$(0,\ 3.757055929263450 \cdot 10^{-1})$	$1.22 \cdot 10^{-15}$
	5	$(0,\ 3.756914213384024 \cdot 10^{-1})$	$9.20 \cdot 10^{-5}$	$(0,\ 3.757055929263451 \cdot 10^{-1})$	$4.60 \cdot 10^{-16}$
$\frac{1}{2}$	2	$(0,\ 3.756045691696934 \cdot 10^{-1})$	$6.56 \cdot 10^{-4}$	$(0,\ 3.757055929263451 \cdot 10^{-1})$	$4.60 \cdot 10^{-16}$
	3	$(0,\ 3.756828289241957 \cdot 10^{-1})$	$1.47 \cdot 10^{-4}$	$(0,\ 3.757055929263451 \cdot 10^{-1})$	$4.60 \cdot 10^{-16}$
	4	$(0,\ 3.757049796804918 \cdot 10^{-1})$	$3.98 \cdot 10^{-6}$	$(0,\ 3.757055929263451 \cdot 10^{-1})$	$4.60 \cdot 10^{-16}$
	5	$(0,\ 3.757055571549585 \cdot 10^{-1})$	$2.32 \cdot 10^{-7}$	$(0,\ 3.757055929263451 \cdot 10^{-1})$	$4.60 \cdot 10^{-16}$

Table 1.— A point y_0 on the boundary of the period annulus $\mathcal{P}$ is computed by the Gauss and HBVM methods of orders 4, 6, 8 and 10 (corresponding to $s = 2, 3, 4, 5$ respectively). By their very nature, if used with a sufficient number of silent stages, HBVMs produce a numerical orbit that precisely lie on the same level set $H(q, p) = H(q_0, p_0)$ as the theoretical one, therefore we see that HBVMs can locate the point y_0 with extreme precision, whatever the order and/or the stepsize used. On the contrary, Gauss methods produce a certain error that may be lowered by reducing the stepsize of integration h and/or by raising their order.

Table 1 compares the results obtained by using the Gauss (HBVM(s,s)) and HBVM(k,s) methods of orders 4, 6, 8 and 10 (therefore, since $s = 2, 3, 4, 5$, we must choose, according to (9), $k = 5, 8, 10, 13$, respectively, in order for the HBVM(k,s) to exactly conserve the Hamiltonian function). We have denoted by $y_0^{(k,s)}$ the point computed by the method HBVM(k,s), and reported the error $|H(y_0^{(k,s)}) - H^*|/H^*$ to estimate the accuracy with which each method computes the boundary of $\mathcal{P}$. As was expected, the accuracy in detecting the right boundary of the period annulus by means of HBVMs is of the same order as the machine precision whatever the order and stepsize used (indeed, the value of $y_0^{(k,s)}$ remains the same for all simulations). On the contrary, the Gauss methods produce a certain error which depends both on the stepsize and on the order used: increasing the accuracy would require a suitable reduction of the stepsize and/or a grow-up of the order. Figure 11 shows that even small oscillations of the numerical Hamiltonian function (left picture) could produce a noticeable irregularity of the numerical orbit in a neighborhood of the boundary of the period annulus (right picture). By their very nature, HBVMs succeed in detecting the set $\partial\mathcal{P}$ with an accuracy of the same order as the machine precision: the error in the Hamiltonian function is negligible (left picture) and the numerical orbit correctly passes through the saddle point P_1.
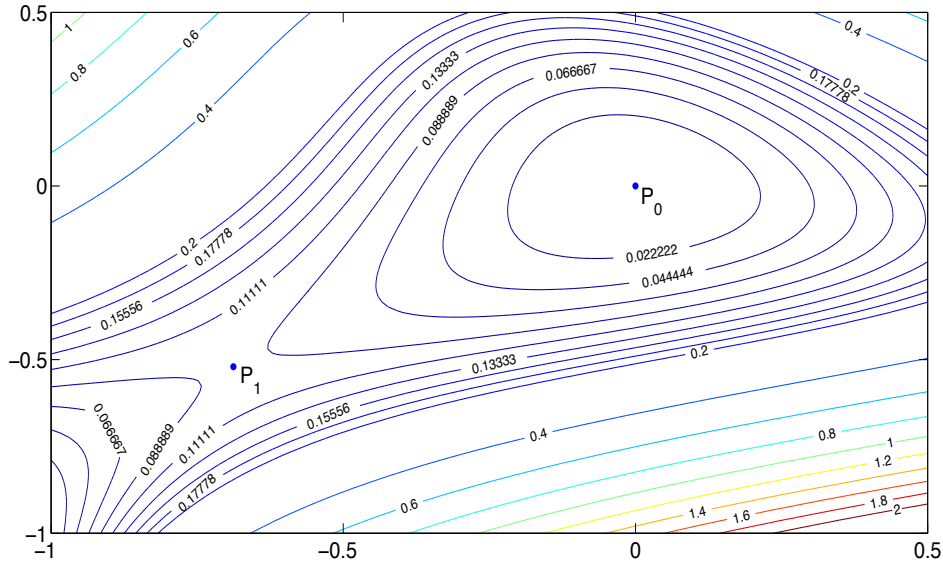
Figure 10.— Level curves of the Hamiltonian (15) in a region that embraces the center point P_0 and the saddle point P_1. Each level curve, corresponding to an orbit of the associated Hamiltonian system, is labeled by a number that indicates its elevation.
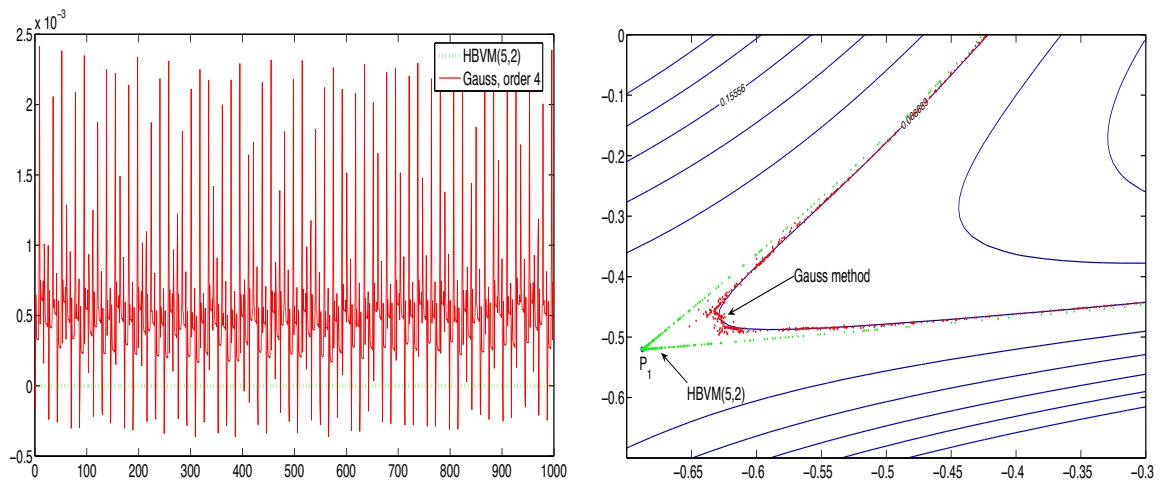

Figure 11.— Left picture: Error $H(q_n, p_n) - H(q_0, p_0)$ in the Hamiltonian function corresponding to the numerical solutions computed by the Gauss method of order 4 and HBVM(5,2) (order 4), with stepsize $h = 1$ and initial conditions $y_0^{(2,2)}$ and $y_0^{(5,2)}$ respectively. Right picture: a closeup of the two numerical orbits in a neighborhood of the saddle point P_1 reveals the difficulty of the Gauss method in detecting the boundary of the period annulus.

References

[1] L. Brugnano, F. Iavernaro, T. Susca. Hamiltonian BVMs (HBVMs): implementation details and applications. "Proceedings of ICNAAM 2009", *AIP Conf. Proc.* **1168** (2009) 723–726.

[2] L. Brugnano, F. Iavernaro, D. Trigiante. Hamiltonian BVMs (HBVMs): a family of 'drift free" methods for integrating polynomial Hamiltonian problems. "Proceedings of ICNAAM

2009", *AIP Conf. Proc.* **1168** (2009) 715–718.

[3] L. Brugnano, F. Iavernaro, D. Trigiante. Analisys of Hamiltonian Boundary Value Methods (HBVMs): a class of energy-preserving Runge-Kutta methods for the numerical solution of polynomial Hamiltonian dynamical systems. *BIT* (2009), submitted. (arXiv:0909.5659)

[4] L. Brugnano, F. Iavernaro, D. Trigiante. Hamiltonian Boundary Value Methods (Energy Preserving Discrete Line Integral Methods). *Jour. of Numer. Anal., Industr. and Appl. Math.* (2009) submitted. (arXiv:0910.3621)

[5] L. Brugnano, F. Iavernaro, D. Trigiante. Isospectral Property of Hamiltonian Boundary Value Methods (HBVMs) and their blended implementation. *BIT* (2010) submitted (arXiv:1002.1387).

[6] L. Brugnano, D. Trigiante. *Solving Differential Problems by Multistep Initial and Boundary Value Methods*, Gordon and Breach Science Publ., Amsterdam, 1998.

[7] C.J. Christopher and C.J. Devlin. Isochronous centers in planar polynomial systems. *SIAM J. Math. Anal.* **28** (1997) 162–177.

[8] A. Cima, A. Gasull and F. Mañosas. Period function for a class of Hamiltonian systems. *J. Differential Equations* **168** (no. 1) (2000) 180–199.

[9] F. Dumortier, J. Llibre and J.C. Artés. *Qualitative theory of planar differential systems. Universitext.* Springer-Verlag, Berlin, 2006.

[10] F. Gustavson. On constructing formal integrals of a Hamiltonian system near an equilibrium point. *Astron. J.* **71** (1966) 670–686.

[11] M. Hénon and C. Heiles. The Applicability of the Third Integral of Motion: Some Numerical Experiments. *Astron. J.* **69** (no. 1) (1964) 73–79.

[12] E. Hairer, C. Lubich, G. Wanner. *Geometric Numerical Integration. Structure-Preserving Algorithms for Ordinary Differential Equations, 2nd ed.*, Springer, Berlin, 2006.

[13] F. Iavernaro, B. Pace. s-Stage Trapezoidal Methods for the Conservation of Hamiltonian Functions of Polynomial Type. *AIP Conf. Proc.* **936** (2007) 603–606.

[14] F. Iavernaro, B. Pace. Conservative Block-Boundary Value Methods for the Solution of Polynomial Hamiltonian Systems. *AIP Conf. Proc.* **1048** (2008) 888–891.

[15] F. Iavernaro, D. Trigiante. On some conservation properties of the Trapezoidal Method applied to Hamiltonian systems. *ICNAAM 2005 proceedings, T.E.Simos, G.Psihoyios, Ch.Tsitouras (Eds.).* Wiley-VCH, Weinheim, 2005, pp. 254–257

[16] F. Iavernaro, D. Trigiante. Discrete conservative vector fields induced by the trapezoidal method. *J. Numer. Anal. Ind. Appl. Math.* **1** (2006) 113–130.

[17] F. Iavernaro, D. Trigiante. State-dependent symplecticity and area preserving numerical methods. *J. Comput. Appl. Math.* **205** no. 2 (2007) 814–825.

[18] F. Iavernaro, D. Trigiante. High-order symmetric schemes for the energy conservation of polynomial Hamiltonian problems. *J. Numer. Anal. Ind. Appl. Math.* **4**,1-2 (2009) 87–111.

[19] J.D. Mireles James. Celestial mechanics notes, Set 1: Introduction to the N-Body Problem. *Available at the url*: http://www.math.utexas.edu/users/jjames/celestMech

[20] X. Jarque, J. Villadelprat. Nonexistence of isochronous centers in planar polynomial Hamiltonian systems of degree four. *J. Differential Equations* **180**, no. 2 (2002) 334–373

[21] X. Jarque, J. Villadelprat. On the period function of centers in planar polynomial Hamiltonian systems of degree four. *Qual. Theory Dyn. Syst.* **3** (no. 1) (2002) 157–180.

[22] J. Llibre and G. Rodríguez. Configurations of limit cycles and planar polynomial vector fields. *J. Differential Equations* **198** (no. 2) (2004) 374–380.